nature research

https://doi.org/10.1038/s41567-020-0990-x

Supplementary information

A strong no-go theorem on the Wigner's friend paradox

In the format provided by the authors and unedited

Supplementary Information:
A strong no-go theorem on the Wigner's friend paradox

Kok-Wei Bong, Aníbal Utreras-Alarcón, Farzad Ghafari, Yeong-Cherng Liang,
Nora Tischler, Eric G. Cavalcanti, Geoff J. Pryde, Howard M. Wiseman

A. WIGNER'S FRIEND THOUGHT EXPERIMENT

In the Wigner's friend thought experiment[1] an observer, whom we call the friend, performs a measurement on a quantum system S. The friend is in a laboratory that can be coherently controlled by a second experimenter called Wigner. As a superobserver, Wigner has the ability to implement arbitrary quantum operations on the friend's laboratory and everything it contains.

Wigner initially assigns a product quantum state $|\phi_0\rangle_F \otimes |\psi_0\rangle_S$ to the overall system composed of the friend, F, and the system, S. For example, the system may be a spin-1/2 particle, and the friend measures the operator corresponding to spin projection along the z direction, with eigenstates $|\uparrow\rangle_S$ and $|\downarrow\rangle_S$.

From Wigner's perspective, the friend's measurement in the z basis is described as a unitary evolution U_Z that correlates the friend (and the display on her measurement apparatus, etc.) to system S in the appropriate way. That is, if the initial state of S is $|\uparrow\rangle_S$, the final state of the joint system is $U_Z(|\phi_0\rangle_F \otimes |\uparrow\rangle_S) = |\text{up}\rangle_F \otimes |\uparrow\rangle_S$, and likewise $U_Z(|\phi_0\rangle_F \otimes |\downarrow\rangle_S) = |\text{down}\rangle_F \otimes |\downarrow\rangle_S$.

An interesting scenario occurs when S is prepared in a superposition state, for example $\frac{1}{\sqrt{2}}(|\uparrow\rangle_S + |\downarrow\rangle_S)$. Then standard textbook quantum mechanics predicts that the friend will observe one or another outcome with equal probability, and the state of the system after measurement (and that of the friend) will be one or another of the corresponding states above. On the other hand, due to the linearity of the unitary map, from Wigner's perspective the final joint state will be $|\Phi^+\rangle_{FS} = \frac{1}{\sqrt{2}}(|\text{up}\rangle_F|\uparrow\rangle_S + |\text{down}\rangle_F|\downarrow\rangle_S)$. This entangled state does not assign well-defined values to the states of S or F separately, and therefore seems to be in direct contradiction with standard textbook quantum mechanics. This contradiction is called the *measurement problem*.

Indeed, if Wigner had the control over F that quantum mechanics in principle allows, then he could measure the POVM $\{|\Phi^+\rangle\langle\Phi^+|_{FS}, I_{FS} - |\Phi^+\rangle\langle\Phi^+|_{FS}\}$, and he would always get the outcome corresponding to state $|\Phi^+\rangle_{FS}$, confirming Wigner's state assignment. Had the state of FS before this measurement been an equal mixture of the post-measurement states $|\text{up}\rangle_F \otimes |\uparrow\rangle_S$ and $|\text{down}\rangle_F \otimes |\downarrow\rangle_S$, Wigner would have obtained, with equal probability, either of the above outcomes.

The contradiction arises from the assumptions that (i) quantum theory is universal and can be applied at any scale, even to a macroscopic observer, and that (ii) there is an objective collapse after a measurement[2]. Thus no contradiction arises if quantum mechanics does not describe objects as large as the friend, or if the collapse of system S is not an objective physical process affecting the wavefunction described by Wigner.

The latter case poses new questions, however. If wavefunction collapse is not objective, is there nevertheless an objective fact corresponding to the friend's observed outcome? Our Theorem 1 demonstrates a contradiction between the (metaphysical) assumptions of No-Superdeterminism, Locality and Absoluteness of Observed Events, and the (empirical) hypothesis that quantum mechanics is valid, and in principle allows coherent operations (such as the above measurements by Wigner) to be implemented, on the scale of a friend F.

B. MAXIMAL QUANTUM VIOLATIONS OF THE GENUINE LF INEQUALITIES

By implementing a see-saw type algorithm (see, e.g., refs.[3–5] and references therein), one finds that the Genuine LF inequality 1 (13), with an LF upper bound of 0, can be violated by quantum correlations up to 1.345 using a partially entangled two-qubit state (with Schmidt coefficients approximately given by 0.776 and 0.631) and rank-1 projective measurements. Moreover, it can be verified by solving a converging hierarchy[6–8] of semidefinite programs that this quantum violation is (within a numerical precision of 10^{-7}) the maximum allowed in quantum theory. In terms of noise robustness, this quantum strategy can tolerate up to 18.3% of white noise before it stops beating the LF bound.

For Genuine LF inequality 2 (14) (with an LF upper bound of 0), the best quantum violation that we have found is 0.880, which apparently can only be achieved using a partially entangled two-qutrit state (with Schmidt coefficients approximately given by 0.645, 0.570, and 0.509) and a combination of rank-2 and rank-1 projectors in the optimal measurements. As with the case of Genuine LF inequality 1, this quantum violation is provably optimal (within a numerical precision of 10^{-7}) using the solution obtained from solving some semidefinite programs. The white-noise tolerance of this inequality is somewhat worse than the other Genuine LF inequality, giving approximately 18.0%.

C. FURTHER INFORMATION ABOUT FIGURE 3

Here, we provide further details on the 2-dimensional slice of the space of correlations presented in Fig. 3. A variant of this figure containing the same slice, but with further salient features added, is shown in Fig. S.1. Any such 2-dimensional slice is spanned by three affinely-independent correlations in this space (see, e.g., ref.[9]). In our case, the chosen slice is spanned by the uniform (white-noise) distribution $\vec{\wp}_0$

$$\wp_0(ab|xy) = \tfrac{1}{4}, \quad \forall\, a, b, x, y, \tag{S.1}$$

an extreme point of the LF polytope:

$$\begin{aligned}\wp_{LF}^{\mathrm{Ext}}(ab|xy) =& \delta_{xy,1}\delta_{a,-1}\delta_{b,1} \\ &+ \tfrac{1}{2}\left[\delta_{x,1}\delta_{a,-1}(1-\delta_{y,1}) + \delta_{y,1}\delta_{b,1}(1-\delta_{x,1})\right] \\ &+ \tfrac{1}{4}\left[1 + (-1)^{xy-x-y}ab\right](1-\delta_{x,1})(1-\delta_{y,1}),\end{aligned} \tag{S.2}$$

and a symmetrical quantum correlation, written in the Collins-Gisin form (see, e.g., Eq. (9) of ref.[10]):

$$\wp_{\mathcal{Q}}^{\text{Max}} : \left[\begin{array}{c|ccc} & 0.554 & 0.409 & 0.537 \\ \hline 0.554 & 0.197 & 0.021 & 0.150 \\ 0.409 & 0.021 & 0.311 & 0.040 \\ 0.537 & 0.150 & 0.040 & 0.109 \end{array}\right], \tag{S.3}$$

i.e., the i-th row of the left-most column represent Alice's marginal probability $\wp_{\mathcal{Q}}^{\text{Max}}(+1|x = i-1)$, the j-column of the top row represent Bob's marginal probability $\wp_{\mathcal{Q}}^{\text{Max}}(+1|y = j-1)$, while the remaining entries at the i-th and j-th column represent the joint probability $\wp_{\mathcal{Q}}^{\text{Max}}(+1,+1|x = i-1, y = j-1)$. The quantum correlation $\vec{\wp}_{\mathcal{Q}}^{\text{Max}}$ is the one that maximally violates Genuine LF inequality 1 (13), giving a value of 1.345, as explained in Sec. B.

In our plot, we have chosen the left-hand side of Eq. (13) to label our horizontal axis, while the vertical axis is labelled by the left-hand side of the Semi-Brukner inequality $-\langle A_2B_1\rangle - \langle A_2B_2\rangle - \langle A_3B_1\rangle + \langle A_3B_2\rangle \geq -2$. Different choices would lead to affine transformations of the plot. Also shown in the figure are a dashed vertical line and a dashed horizontal line intersecting at $\vec{\wp}_{LF}^{\text{Ext}}$. These dashed lines mark a projection of the boundary of the LF polytope—as given by inequality (13) and a relabeling of inequality (18) to give a lower bound of -2 as allowed by LF correlations—on the plane that we have chosen. Note also that the set of LHV correlations (coloured green in the figure) could also touch this boundary of -2, but this does not take place on the 2-dimensional plane that we have chosen.

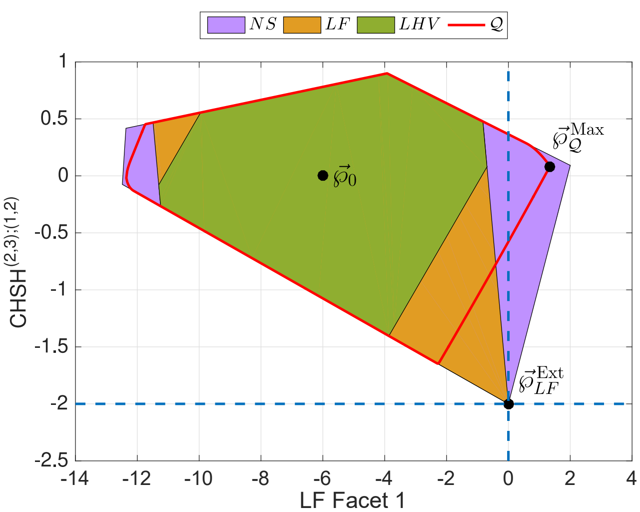

Fig.S.1. **Detailed version of Fig. 3 from the main text.** The 2-dimensional slice of the space of correlations is the same as in Fig. 3. This slice is spanned by the three points $\wp_0$, $\wp_{LF}^{\text{Ext}}$, and $\wp_{\mathcal{Q}}^{\text{Max}}$, defined in Eqs. (S.1), (S.2), and (S.3), respectively. The horizontal axis labels the left-hand side of Eq. (13) whereas the vertical axis denoted by CHSH$^{(2,3);(1,2)}$ is a short hand for the Bell expression appearing in a Semi-Brukner inequality $-\langle A_2B_1\rangle - \langle A_2B_2\rangle - \langle A_3B_1\rangle + \langle A_3B_2\rangle$. Accordingly, the blue dashed lines demarcate the intersection of the boundary of these facets (each representing a half space) with this 2-dimensional slice. In other words, the LF polytope (even beyond this 2-dimensional slice) has to lie above the horizontal dashed line and to the left of the vertical dashed line.

D. EXPERIMENTAL QUANTUM STATES

We obtain the experimental quantum states through tomographic state reconstruction based on maximum-likelihood estimation. For each experimental state ρ_{exp}, the highest Uhlmann–Jozsa fidelity[11] $\left[\mathrm{Tr}\left(\sqrt{\sqrt{\rho_{\text{exp}}}\rho_\mu\sqrt{\rho_{\text{exp}}}}\right)\right]^2$ with the family of states ρ_μ is provided in Table S.I, along with the corresponding best μ value. Uncertainties represent ± 1 standard deviations, estimated based on Monte Carlo simulations using 100 samples of Poisson-distributed photon counts.

μ-parameter	Fidelity
0.992 ± 0.002	0.9789 ± 0.0007
0.921 ± 0.002	0.9883 ± 0.0007
0.866 ± 0.002	0.9887 ± 0.0007
0.809 ± 0.002	0.9868 ± 0.0007
0.798 ± 0.002	0.9873 ± 0.0007
0.744 ± 0.002	0.9824 ± 0.0007

TABLE S.I. Characterization of the six experimental states with respect to the family of target states.

[1] Wigner, E. P. Remarks on the mind-body question. In Good, I. J. (ed.) *The Scientist Speculates*, 284–302 (Heinemann, London, 1961).

[2] Baumann, V. & Wolf, S. On formalisms and interpretations. *Quantum* **2**, 99 (2018).

[3] Pál, K. F. & Vértesi, T. Quantum bounds on Bell inequalities. *Phys. Rev. A* **79**, 022120 (2009).

[4] Liang, Y.-C., Lim, C.-W. & Deng, D.-L. Reexamination of a multisetting Bell inequality for qudits. *Phys. Rev. A* **80**, 052116 (2009).

[5] Liang, Y.-C. & Doherty, A. C. Bounds on quantum correlations in Bell-inequality experiments. *Phys. Rev. A* **75**, 042103 (2007).

[6] Navascués, M., Pironio, S. & Acín, A. Bounding the set of quantum correlations. *Phys. Rev. Lett.* **98**, 010401 (2007).

[7] Navascués, M., Pironio, S. & Acín, A. A convergent hierarchy of semidefinite programs characterizing the set of quantum correlations. *New J. Phys.* **10**, 073013 (2008).

[8] Doherty, A. C., Liang, Y.-C., Toner, B. & Wehner, S. The quantum moment problem and bounds on entangled multi-prover games. In *Proceedings of the 2008 IEEE 23rd Annual Conference on Computational Complexity*, CCC '08, 199–210 (IEEE Computer Society, Washington, DC, USA, 2008).

[9] Goh, K. T. *et al.* Geometry of the set of quantum correlations. *Phys. Rev. A* **97**, 022104 (2018).

[10] Collins, D. & Gisin, N. A relevant two qubit Bell inequality inequivalent to the CHSH inequality. *J. Phys. A: Math. Gen.* **37**, 1775–1787 (2004).

[11] Liang, Y.-C. *et al.* Quantum fidelity measures for mixed states. *Rep. Prog. Phys* **82**, 076001 (2019).